Cancer Science
Japanese Cancer Association JCA
Open Access

A role of uridylation pathway for blockade of let-7 microRNA biogenesis by Lin28B

Hiroshi I. Suzuki,[1,2] Akihiro Katsura[2] and Kohei Miyazono[2]

[1]David H. Koch Institute for Integrative Cancer Research, Massachusetts Institute of Technology, Cambridge, Massachusetts, USA; [2]Department of Molecular Pathology, Graduate School of Medicine, The University of Tokyo, Tokyo, Japan

Key words
Biogenesis, Dis3l2, let-7, Lin28B, MCPIP1

Correspondence
Hiroshi I. Suzuki, Koch Institute for Integrative Cancer Research, Massachusetts Institute of Technology, 500 Main St., 76-417, Cambridge, MA 02139, USA.
Tel: 617-253-6457; Fax: 617-253-3867;
E-mail: hisuzuki@mit.edu

Funding Information
Japan Society for the Promotion of Science; Ministry of Education, Culture, Sports, Science, and Technology of Japan; Cell Science Research Foundation.

Received May 1, 2015; Revised June 2, 2015; Accepted June 8, 2015

Cancer Sci **106** (2015) 1174–1181

doi: 10.1111/cas.12721

The precise control of microRNA (miRNA) biosynthesis is crucial for gene regulation. Lin28A and Lin28B are selective inhibitors of biogenesis of let-7 miRNAs involved in development and tumorigenesis. Lin28A selectively inhibits let-7 biogenesis through cytoplasmic uridylation of precursor let-7 by TUT4 terminal uridyl transferase and subsequent degradation by Dis3l2 exonuclease. However, a role of this uridylation pathway remains unclear in let-7 blockade by Lin28B, a paralog of Lin28A, while Lin28B is reported to engage a distinct mechanism in the nucleus to suppress let-7. Here we revisit a functional link between Lin28B and the uridylation pathway with a focus on let-7 metabolism in cancer cells. Both Lin28A and Lin28B interacted with Dis3l2 in the cytoplasm, and silencing of Dis3l2 upregulated uridylated pre-let-7 in both Lin28A- and Lin28B-expressing cancer cell lines. In addition, we found that amounts of let-7 precursors influenced intracellular localization of Lin28B. Furthermore, we found that MCPIP1 (Zc3h12a) ribonuclease was also involved in degradation of both non-uridylated and uridylated pre-let-7. Cancer transcriptome analysis showed association of expression levels of Lin28B and uridylation pathway components, TUT4 and Dis3l2, in various human cancer cells and hepatocellular carcinoma. Collectively, these results suggest that cytoplasmic uridylation pathway actively participates in blockade of let-7 biogenesis by Lin28B.

Let-7 family miRNAs are highly conserved miRNAs that regulate normal development and function as potent tumor suppressors. MiRNAs, including let-7, are generated by stepwise processing by two ribonucleases.[1,2] Nuclear RNase III Drosha cleaves primary transcripts of miRNA (pri-miRNAs) to yield the hairpin-structure precursor miRNAs (pre-miRNAs). Pre-miRNAs are exported to the cytoplasm and further processed to miRNA duplexes by the cytosolic RNase III Dicer. From miRNA duplexes, a single RNA strand is incorporated into Argonaute proteins, leading to formation of RNA-induced silencing complex. Functions of let-7 are tightly regulated through inhibition of the biogenesis thereof by conserved RNA-binding proteins Lin28 in diverse species.[3–7] In mammals, two Lin28 paralogues, Lin28 (Lin28A) and Lin28B, are known to selectively suppress let-7 biogenesis.[3–6] Lin28A is reported to be expressed in embryonic stem (ES) cells and embryonic carcinoma cells. In contrast, Lin28B is found in placenta, testis and fetal liver.[8] Lin28 proteins are also known as reprogramming factors, which cooperate with Oct4, Sox2 and Nanog,[9] and regulators of tumor progression.[10–12]

In a series of studies in ES cells and embryonic cells endogenously expressing Lin28A, it has been shown that cytoplasmic Lin28A binds to the terminal loop of precursor let-7 (pre-let-7), induces 3′-terminal oligouridylation of pre-let-7 by terminal uridyl transferase (TUTase) TUT4 (Zcchc11), and blocks pre-let-7 processing by Dicer, thereby inhibiting let-7 biogenesis.[6,13–16] Another TUTase TUT7 (Zcchc6) is reported to have a redundant function with TUT4.[13,16] Uridylated pre-let-7 is labile and was recently shown to be degraded by Dis3l2 exonuclease.[17,18] In contrast, Lin28 proteins have been reported to have a capacity to interfere with Drosha processing of primary transcripts of let-7 (pri-let-7).[3,4,19] A recent study reports that Lin28A and Lin28B use distinct molecular machineries to inhibit let-7: Lin28A recruits cytoplasmic uridylation pathway, but Lin28B mainly inhibits Drosha processing of pri-let-7 in the nucleus.[20] However, several studies suggest that Lin28A and Lin28B have similar biochemical properties and involve similar mechanisms to inhibit let-7.[6,13,21] Therefore, the role of the uridylation pathway in let-7 blockade by Lin28B remains unclear. In this study, we perform comparative analyses of Lin28A and Lin28B and revisit a functional link between Lin28B and the uridylation pathway together with an inquiry into the association between Lin28 and uridylation pathway components in cancer transcriptomes.

Materials and Methods

Cell lines, antibodies and plasmids. HEK293T, HeLa, HepG2, T47D, A549 and PANC-1 cell lines were obtained from the American Type Culture Collection and maintained in DMEM (GIBCO, Gaithersburg, MD, USA) containing 10% FBS, except for T47D cells. T47D cells were maintained in RPMI1640 medium (GIBCO) with 10 μg/mL insulin and 10% FBS. The following antibodies were used: Flag epitope tag M2 (Sigma, St. Louis, MO, USA); HA epitope tag Y11 (Santa Cruz); HDAC1 H-51 (Santa Cruz, Santa Cruz, CA, USA); and

© 2015 The Authors. Cancer Science published by Wiley Publishing Asia Pty Ltd on behalf of Japanese Cancer Association.
This is an open access article under the terms of the Creative Commons Attribution-NonCommercial License, which permits use, distribution and reproduction in any medium, provided the original work is properly cited and is not used for commercial purposes.

α-tubulin DM-1A (Sigma). cDNAs encoding human Dis3l2, Lin28A and Lin28B were cloned into pcDNA3 vector. GFP-Lin28A and GFP-Lin28B expression vectors were constructed by inserting Lin28A and Lin28B cDNAs to pEGFP-C1 (Clontech, Mountain View, CA, USA). Pri-let-7g expression vector and let-7g sensor vector were generated according to our previous reports.[22–25] The primer sequences used are shown in Supplementary Table S1.

siRNA. Control siRNAs and siRNAs for Dis3l2 and MCPIP1 were purchased from Dharmacon (Lafayette, CO, USA; SMARTpool) and Invitrogen (Carlsbad, CA, USA). siRNAs were introduced into cells using DharmaFECT 1 or 2 transfection reagent (Dharmacon) or Lipofectamine RNAiMAX (Invitrogen). RNAs were collected for subsequent experiments after 48–72 h.

Fluorescence microscopy. After transfection with GFP-Lin28A and GFP-Lin28B expression vectors, cells were observed by Olympus IX70 fluorescence microscope.

Immunoblot and luciferase reporter assay. Cytoplasmic and nuclear fractions were extracted using NE-PER Nuclear and Cytoplasmic Extraction Reagent (Pierce, Rockford, IL, USA). Immunoprecipitation, immunoblot analysis and luciferase reporter assay were performed as previously described.[22]

Quantitative RT-PCR assays. qRT-PCR assays were performed as previously described.[22–25] Total RNAs were extracted by using Trizol (Invitrogen) or a miRNeasy Mini Kit (Qiagen, Valencia, CA, USA). For detection of mRNA, pri-let-7g and U6, total RNAs were subjected to reverse transcription using random hexamers and a PrimeScript II First Strand cDNA Synthesis Kit (Takara, Shiga, Japan) and quantitative RT-PCR (qRT-PCR) assay. Mature miRNAs were detected using a TaqMan MicroRNA assay kit (Applied Biosystems, Foster City, CA, USA). For detection of pre-let-7g, small RNA fraction was purified with the miRNeasy Mini Kit (Qiagen), and subjected to reverse transcription using the PrimeScript II First Strand cDNA Synthesis Kit. To evaluate the expression levels of uridylated pre-let-7g, total RNA was subjected to reverse transcription using oligo$(dA)_{12}$ and the SuperScript III First-Strand Synthesis System (Invitrogen; 60 min at 50°C) according to the previous report.[17] qRT-PCR was performed using the 7500 Fast Real-Time PCR System and StepOne Real-Time PCR System (Applied Biosystems). Results were normalized to GAPDH for mRNA and pri-let-7g detection, and U6 snRNA or RNU44 snoRNA for evaluation of pre-let-7, mature let-7 and uridylated pre-let-7. The primer sequences are described in Supplementary Table S1.

Northern blot analyses and pre-miRNA decay assay. Northern blot analysis was carried out as previously described.[22,23] γ^{32}P-ATP-labeled oligonucleotides complementary to miRNAs were used as probes. U6 snRNA was used as a control for quantification. The stability of uridylated pre-let-7 was assessed using the Tet-Off Advanced Inducible Gene Expression System (Clontech). pTRE-Tight-pri-let-7g was constructed by inserting pri-let-7g into pTRE-Tight vector (Clontech). HepG2 cells with pTet-off Advanced vector (Clontech) were

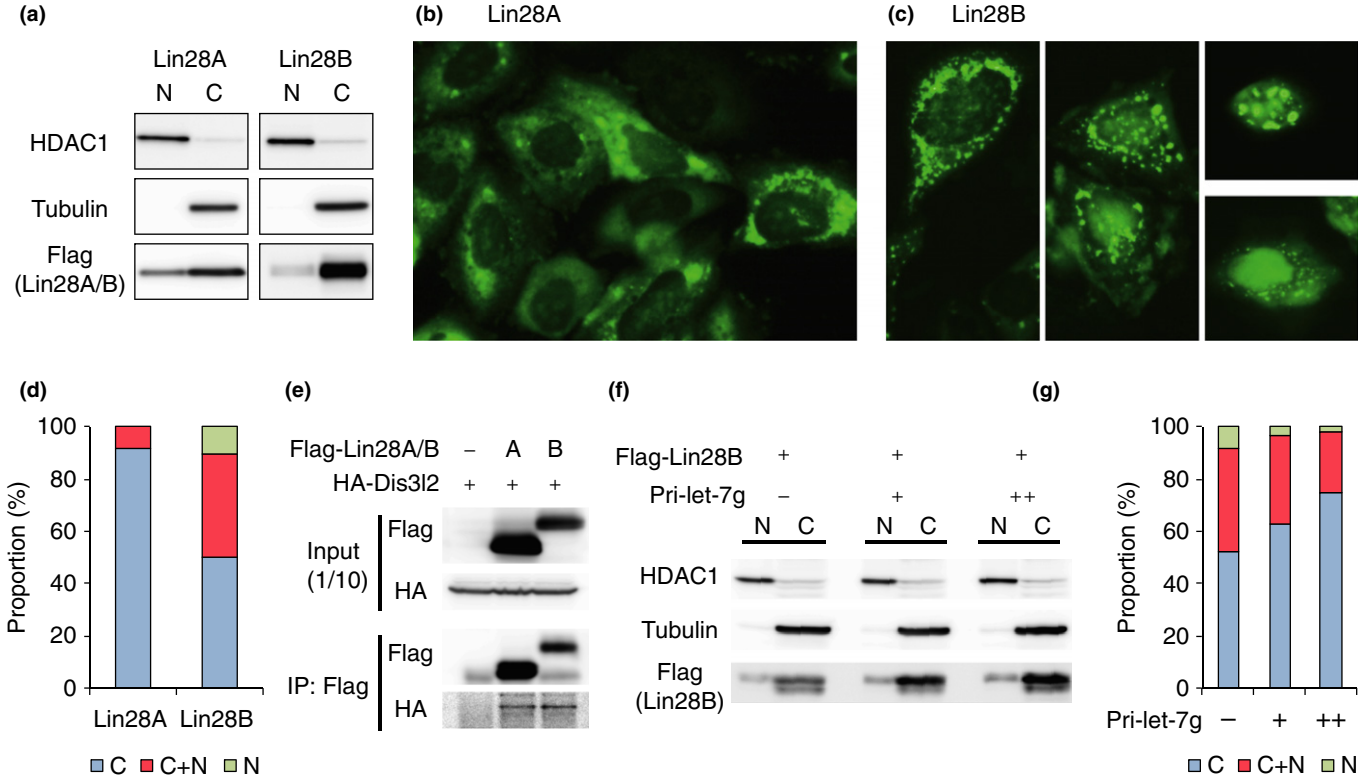

Fig. 1. Subcellular localization of Lin28B and its interaction with Dis3l2. (a) Localization of Lin28A and Lin28B. HEK293T cells were transfected with Flag-Lin28A/B expression vectors, and applied to subcellular fractionation and immunoblotting. (b,c) Localization of GFP-Lin28A and GFP-Lin28B. In panels (b) and (c), GFP-Lin28A (b) and GFP-Lin28B (c) were ectopically expressed in HeLa cells and GFP distribution was microscopically observed. (d) Localization profiles of Lin28A and Lin28B were scored as cytoplasmic (C), cytoplasmic and nuclear (C+N) or nuclear (N). For Lin28B, various patterns of GFP distribution were observed. (e) Interaction between Lin28A/B and Dis3l2. Flag-Lin28A/B and HA-Dis3l2 were ectopically expressed in HEK293T cells. Cell lysates were immunoprecipitated with anti-Flag antibody, followed by immunoblotting. (f, g) Effect of pri-let-7g overexpression on Lin28B localization. Flag-Lin28B (f) or GFP-Lin28B (g) and pri-let-7g were expressed in HeLa cells and analyzed by subcellular fractionation and immunoblotting (f) and microscopic analysis (g), respectively.

© 2015 The Authors. Cancer Science published by Wiley Publishing Asia Pty Ltd on behalf of Japanese Cancer Association.

transfected with pTRE-Tight–pri-let-7g and control siRNA or siRNA for MCPIP1. At 48 h post-transfection, pri-let-7g transcription was halted by addition of doxycycline (DOX) (1 μg /mL). Total RNA was extracted at the indicated time periods and subjected to northern blot analysis.

Gene expression profiling analysis. Gene expression profiling data of Cancer Cell Line Encyclopedia (CCLE) have been described previously.[26] mRNA expression and miRNA expression data for hepatocellular carcinoma patient samples were downloaded from The Cancer Genome Atlas (TCGA) Data Portal (https://tcga-data.nci.nih.gov/tcga/) in May 2014. We used level-3 pre-interpreted data provided by TCGA. Gene Set Enrichment Analysis (GSEA) was performed with GSEA software available from the Broad Institute (http://www.broadinstitute.org/gsea/).[27] C3MIR, C2CGP and Hallmark gene sets were used. High confidence let-7 target genes have been described previously.[28]

Statistical analysis. Statistical analysis was performed using the two-tailed Student's *t*-test for RT-PCR analyses and the Wilcoxon signed rank sum test for gene expression analyses in CCLE and TCGA databases.

Results

Cytoplasmic localization of Lin28B and the interaction with Dis3l2. To investigate the relationship between Lin28B and the uridylation pathway, we first intensively compared molecular features of Lin28A and Lin28B. Subcellular fractionation and immunoblot analyses confirmed the predominant cytoplasmic localization of both Lin28A and Lin28B (Fig. 1a), which was consistent with previous observations on cytoplasmic localization of Lin28B.[5,8,21,29,30] Subcellular localization of GFP-tagged Lin28A and Lin28B was consistent with this finding (Fig. 1b–d). GFP-Lin28A localized to the cytoplasm, especially the perinuclear area (Fig. 1b), whereas Lin28B distributed in both the nuclei and cytoplasm in constant populations of transfected cells and sometimes in the nucleoli (Fig. 1c,d). Dis3l2 has been reported to localize primarily in the cytoplasm.[17,31,32] Next, we investigated whether cytoplasmic Lin28B interacts with Dis3l2 exonuclease, similarly to Lin28A.[17] Immunoprecipitation analyses revealed that both Lin28A and Lin28B interact with Dis3l2 to a similar extent (Fig. 1e). In addition, we investigated whether amounts of coexisting let-7 precursors modulate Lin28B localization. Interestingly, we found that increased expression of let-7 precursors by pri-let-7 overexpression may promote cytoplasmic shift of Lin28B (Fig. 1f,g).

Silencing of Dis3l2 upregulates uridylated pre-let-7 in both Lin28A-expressing and Lin28B-expressing cancer cells. Based on the interaction between Lin28B and Dis3l2, we next sought a possibility that Dis3l2 is involved in Lin28B-mediated let-7 inhibition through degradation of uridylated pre-let-7. Lin28A and Lin28B are reported to be expressed in various cancer cell lines.[33–35] To this end, we validated the expression of Lin28A and Lin28B in several cancer cell lines and confirmed that Lin28B is expressed in A549 lung cancer, HepG2 hepatoma and PANC-1 pancreatic cancer cell lines, whereas Lin28A is expressed in T47D breast cancer cells (Fig. 2a). This expression pattern is consistent with the mutual exclusive expression patterns of Lin28A and Lin28B in cancer cells.[20] Next, we suppressed the expression levels of Dis3l2 in these cells and examined the expression levels of uridylated pre-let-7 to prove a direct link between Lin28-Dis3l2 axis and let7 uridylation. Using oligo(dA) primer, we reverse transcribed RNA containing oligouridine tails and performed qRT-PCR analysis for let-7

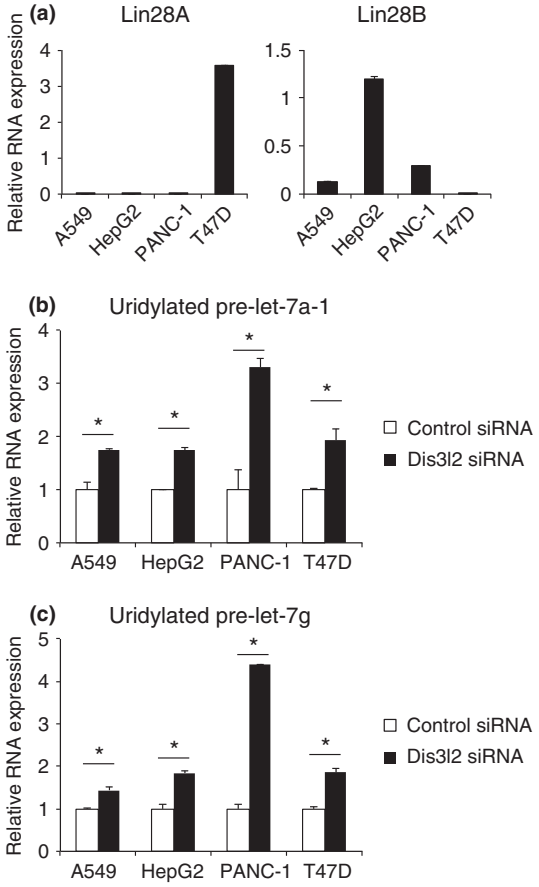

Fig. 2. Silencing of Dis3l2 upregulates uridylated pre-let-7 in both Lin28A- and Lin28B-expressing cancer cells. (a) Expression levels of Lin28A and Lin28B in human cancer cell lines, quantified by quantitative RT-PCR (qRT-PCR) analysis. (b, c) Effects of Dis3l2 depletion on the levels of uridylated pre-let-7. The levels of uridylated pre-let-7a-1 (b) and pre-let-7g (c) were compared by qRT-PCR analyses in cells transfected with control siRNA or siRNA for Dis3l2. RNA expression levels of cells transfected with control siRNA were set at 1. Error bars represent SD. $*P < 0.05$

precursors. In a similar manner with the effects of Dis3l2 silencing in Lin28A-expressing ES cells,[17] silencing of Dis3l2 upregulated the expression levels of uridylated pre-let-7a-1 and pre-let-7g in both Lin28A-expressing and Lin28B-expressing cancer cells (Fig. 2b,c). Thus, these findings indicate that the uridylation pathway lies directly beneath both Lin28A and Lin28B.

Involvement of MCPIP1 in Lin28-controlled let-7 biogenesis. Multiple studies have identified various RNA-binding proteins as regulators of miRNA biogenesis. We have previously identified MCPIP1 (also known as Zc3h12a) as a potent suppressor of miRNA activity and production.[22,36] MCPIP1 cleaves the terminal loops of pre-miRNAs and blocks miRNA biogenesis. We previously reported that MCPIP1 is expressed in HepG2 cells expressing Lin28B and that silencing of MCPIP1 led to widespread upregulation of miRNAs in this cell type.[22] Considering that both Lin28B and MCPIP1 can be induced by inflammatory signals along with activation of NF-κB pathway,[37–39] we additionally investigated the roles of MCPIP1 in let-7 biogenesis in the context of crosstalk with the uridylation pathway.

We first investigated whether MCPIP1 suppresses the ordinary course of let-7 maturation and let-7 function. In accordance with our previous results, MCPIP1 potently suppressed the activities

© 2015 The Authors. Cancer Science published by Wiley Publishing Asia Pty Ltd on behalf of Japanese Cancer Association.

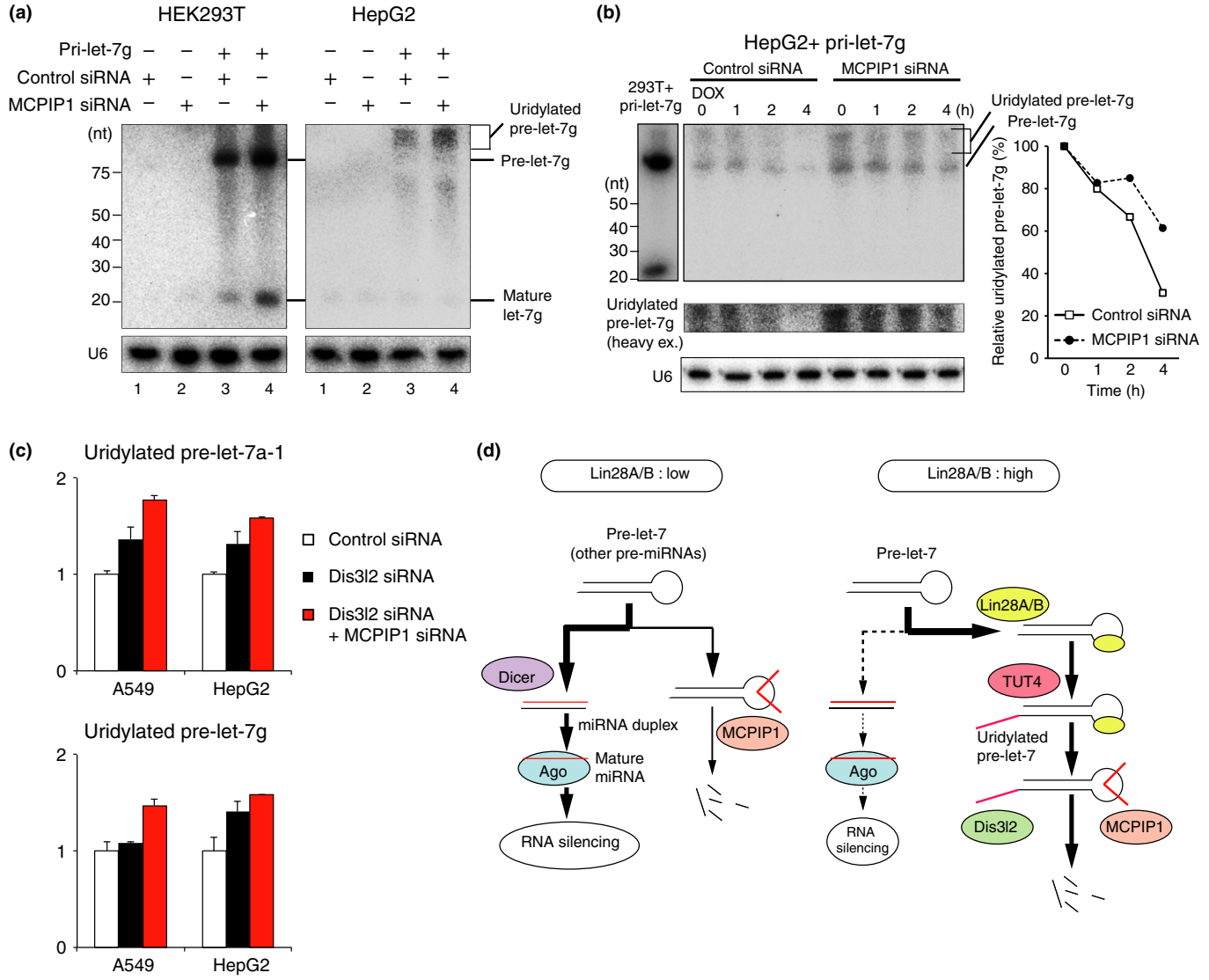

Fig. 3. Involvement of MCPIP1 in let-7 biogenesis. (a) Cell-type-dependent differences in intracellular pre-let-7g fate. Northern blot analyses were performed to determine let-7 maturation after transfection of pri-let-7g and *MCPIP1* siRNA in HEK293T and HepG2 cells. (b) MCPIP1 promotes the decay of uridylated pre-let-7g. HepG2 cells expressing pri-let-7g in a tetracycline-repressive manner were transfected with control siRNA or MCPIP1 siRNA, and subjected to northern blot analysis to evaluate the decay of pre-let-7g after doxycycline (DOX) treatment. Uridylated pre-let-7g was quantified and normalized to U6 in the right. (c) Roles of endogenous MCPIP1 in degradation of uridylated pre-let-7. Cells were transfected with control siRNA or siRNA for Dis3l2 and MCPIP1, and subjected to qRT-PCR analysis. Error bars represent SD. (d) A schematic model for the regulation of let-7 biogenesis by Lin-28, TUT4, Dis3l2 and MCPIP1. In the presence of Lin-28, the pre-let-7 is predominantly bound to Lin-28, uridylated by TUT4, further degraded by Dis3l2 and MCPIP1.

of let-7g, depending on intact NYN nuclease domain and CCCH motif, in HEK293T cells (Suppl. Fig. S1a). MCPIP1 suppressed *de novo* biogenesis of let-7g (Suppl. Fig. S1b). These results were confirmed by northern blot analysis in HEK293T cells (Fig. 3a, left).

In contrast, in HepG2 cells, the introduction of pri-let-7g could not achieve the production of pre-let-7g and mature let-7g (Fig. 3a, right). In addition, products slightly longer than expected pre-let-7g were observed (Fig. 3a, right), indicating effective pre-let-7 uridylation triggered by Lin28B. In this condition, intriguingly, MCPIP1 knockdown further promoted the accumulation of uridylated pre-let-7 in HepG2 cells (Fig. 3a, right). We examined whether MCPIP1 promotes the degradation rate of uridylated pre-let-7, using a tetracycline-regulated repression system. As shown in Figure 3(b), MCPIP1 knockdown attenuated the decay of uridylated pre-let-7 after a halt of pri-let-7g transcription by DOX treatment. Combination of silencing of Dis3l2 and MCPIP1 further enhanced the expression levels of uridylated pre-let-7 in A549 and HepG2 cells (Fig. 3c). These results thus suggest that MCPIP1 is a secondary ribonuclease involved in degradation of uridylated pre-let-7 (Fig. 3d).

Association of Lin28A/B and uridylation pathway components in cancer cells. Lin28 proteins are known to contribute to tumor progression.[40] Overexpression of Lin28A and Lin28B (overall frequency 10–30%) is observed in diverse cancer types, including germ-cell tumors, leukemia, breast cancer, colon cancer, hepatocellular carcinoma, neuroblastoma, Wilms tumor and ovarian cancer.[20,33–35,40,41] In particular, high expression of Lin28B is reported in liver cancer and neuroblastoma.[33,42,43] In these cancer types, Lin28A and Lin28B are thought to promote tumor progression and to be associated with advance

© 2015 The Authors. Cancer Science published by Wiley Publishing Asia Pty Ltd on behalf of Japanese Cancer Association.

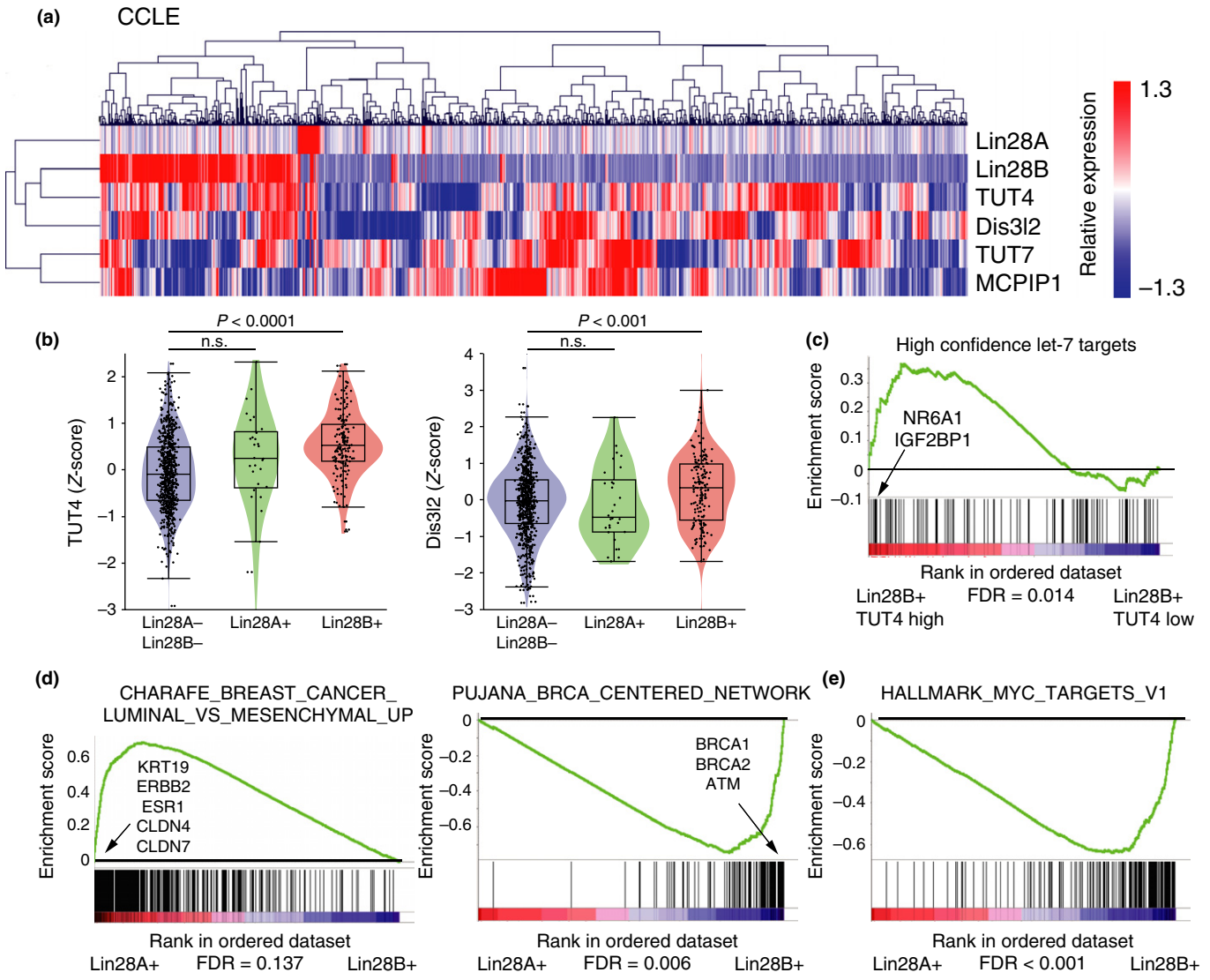

Fig. 4. An association between Lin28 and uridylation pathway components in cancer cell lines. (a) Heat map showing the expression of Lin28A, Lin28B, TUT4, TUT7, MCPIP1 and Dis3l2 in Cancer Cell Line Encyclopedia (CCLE) cancer cell line database. (b) Violin plot of Z-score for expression levels for TUT4 and Dis3l2 in CCLE cancer cell line database. (c) Upregulation of let-7 high confidence target genes in TUT4-high Lin28B-positive cell lines in CCLE, compared to TUT4-low Lin28B-positive cell line, analyzed by GSEA. (d, e) GSEA analysis in CCLE dataset using C2CGP gene sets (d) and Hallmark gene sets (e). The results show that genes upregulated in luminal-like breast cancer cell lines compared to the mesenchymal-like cell lines (left) and BRCA network-related genes (right) are enriched in Lin28A-positive and Lin28B-positive cancer cell lines, respectively (d). Hallmark gene set analysis also shows enrichment of Myc target genes in Lin28B-positive cancer cell lines (e).

stages.[33,35,40,42] Next, we investigated the association between Lin28A/B and the components of uridylation pathway. To this end, we used the CCLE database, which includes genome-wide expression profiles of diverse cancer cell line cohorts.[26] Clustering analysis of expression profiles for Lin28A, Lin28B, TUT4, TUT7, Dis3l2 and MCPIP1 showed that a subset of cancer cell lines expressed Lin28A and Lin28B in a mutually exclusive manner and that Lin28B-positive cancer cells tended to show high expression of TUT4 and Dis3l2 (Fig. 4a). In contrast, we failed to observe a clear tendency for high expression of TUT7 and MCPIP1 in Lin28B-positive cancer cells, although a subset of Lin28B-positive cancer cells, including A549 and HepG2 cells, showed high expression of MCPIP1. Further analyses showed significantly high expression of TUT4 and Dis3l2 in Lin28B-positive, but not Lin28A-positive, cancer cells (Fig. 4b). We also investigated the association between TUT4 expression status and let-7 function. Because the CCLE database does not include miRNA expression profiles, we interrogated let-7 function using GSEA[27] for let-7 potential targets predicted by TargetScan and high confidence let-7 target genes, which were recently reported.[28] GSEA confirmed derepression of let-7 potential targets and high confidence targets in both Lin28A-positive and Lin28B-positive cancer cells (Suppl. Fig. S2a,b). Moreover, we found that TUT4-high Lin28B-positive cancer cells showed high expression of high confidence let-7 targets compared to TUT4-low Lin28B-positive cancer cells, while only a marginal increase was observed for let-7 potential targets (Fig. 4c and Suppl. Fig. S2c). Derepressed targets in TUT4-high Lin28B-positive cancer cells included some oncofetal genes, including IGF2BP1 and NR6A1, an embryonic transcriptional repressor, which is a key target of let-7 for continual suppression of mid-gestation devel-

© 2015 The Authors. Cancer Science published by Wiley Publishing Asia Pty Ltd on behalf of Japanese Cancer Association.

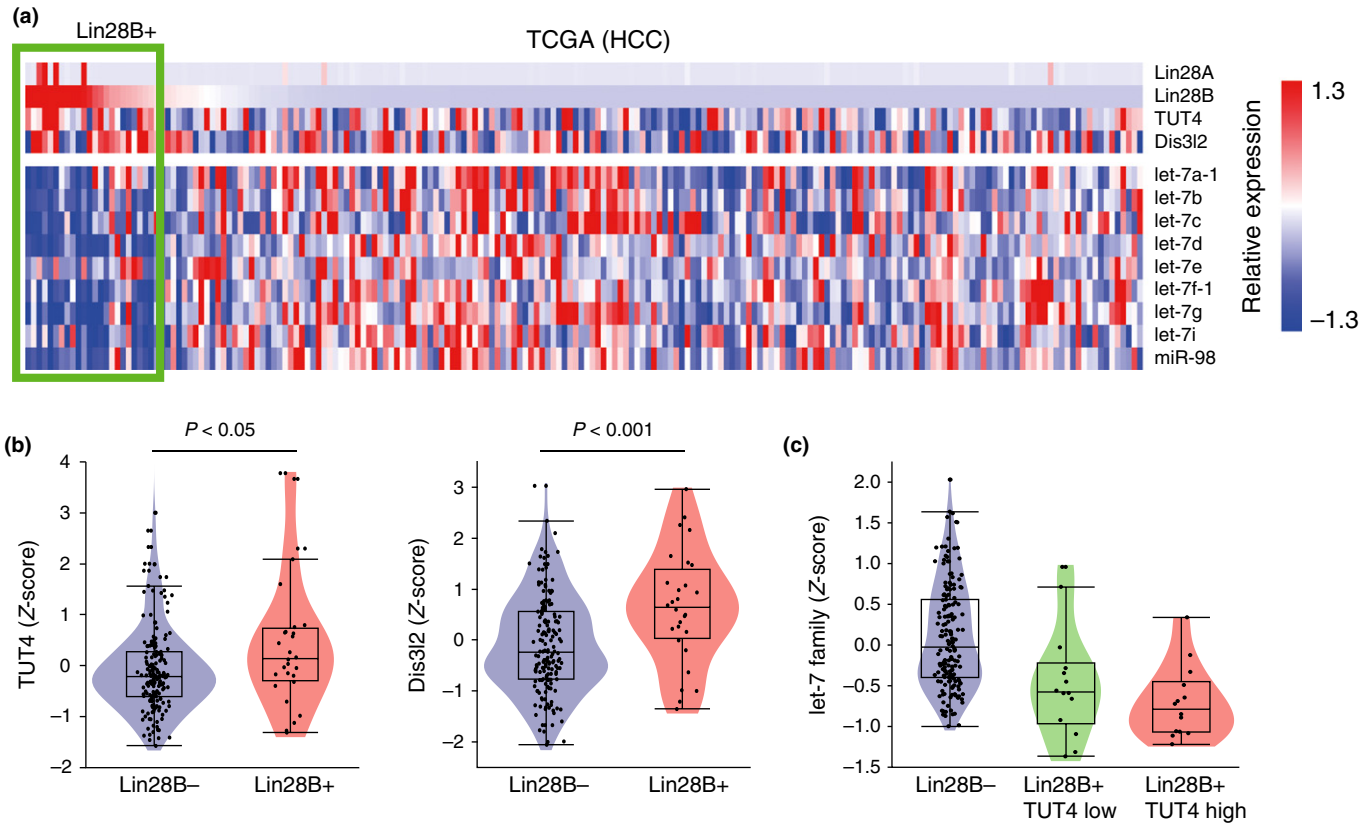

Fig. 5. An association between Lin28 and uridylation pathway components in hepatocellular carcinoma. (a) Heat map showing the expression of Lin28A, Lin28B, TUT4, Dis3l2 and let-7 family miRNAs in TCGA hepatocellular carcinoma (HCC) database. 200 HCC samples were ordered according to Lin28B expression. (b, c) Violin plots of Z-scores for expression levels for TUT4, Dis3l2 (b) and let-7 family miRNAs (c) in TCGA hepatocellular carcinoma database. Boxes represent the median and interquartile range (IQR). Error bars represent 1.5× IQR.

opmental program (Suppl. Table S2).[28] These findings suggest that high expression of TUT4 confers more robust suppression of let-7 functions in Lin28B-positive cancer cells.

We also analyzed characteristics of Lin28A-positive and Lin28B-positive cancer cell lines using the CCLE database. GSEA showed enrichment of genes highly expressed in luminal-type breast cancers,[44] such as KRT19, ERBB2, ESR1, CLDN4 and CLDN7, and BRCA network-related genes (BRCA1, BRCA2 and ATM)[45] in Lin28A-positive and Lin28B-positive cancer cells, respectively (Fig. 4d and Suppl. Table S3). These findings may correlate with a previous study describing that Lin28A is expressed in HER2-positive breast tumors, while Lin28B is expressed in triple-negative breast tumors.[20] In addition, Myc is reported to transcriptionally activate Lin28B but not Lin28A,[46] and GSEA also suggested high activity of Myc in Lin28B-positive cancer cells (Fig. 4e and Suppl. Table S4). Collectively, these findings suggest that Lin28A and Lin28B may be involved in tumor progression in distinct cellular contexts and converge on overlapped molecular machineries to inhibit let-7.

Lin28B and uridylation pathway in hepatocellular carcinoma. We investigated the association between Lin28B and uridylation pathway in another dataset for human hepatocellular carcinoma (HCC), provided by the TCGA. The TCGA database of 200 HCC samples includes approximately 15% of Lin28B-positive cases, while Lin28A-positive cases were scanty. This dataset also showed a trend of Lin28B-positive cancer showing high expression of TUT4 and Dis3l2 (Fig. 5a), similar to the CCLE dataset. High expression of TUT4 and Dis3l2 in Lin28B-positive was statistically significant (Fig. 5b). In addition, we interrogated the association between TUT4 expression status and let-7 expression status to examine direct impacts of TUT4 on let-7 biogenesis, by analyzing paired profiles for RNA and miRNA in the TCGA database (Fig. 5a) and averaging let-7 family expression values. This analysis showed that TUT4 high cases tended to express low levels of let-7 families, although this did not reach statistical significance and should be confirmed by further large-scale investigations (Fig. 5c). In addition, a recent report suggests that the extent of let-7 blockade by Lin28 proteins depends on the length and sequence feature of pre-let-7 of independent let-7 miRNAs.[21] Accordingly, we observed a trend that let-7 members with long uridine-rich terminal loops (let-7b, let-7d, let-7f, let-7g, let-7i and miR-98) decreased more remarkably in Lin28-positive cases, than let-7 members with short terminal loops (let-7a, let-7c and let-7e) (Suppl. Fig. S3). Together with the results in Figure 4(c), these findings suggest that high TUT4 expression promotes inhibition of let-7 in Lin28B-positive cancers.

Discussion

In summary, we revisited a functional link between Lin28B and the uridylation pathway and found that both Lin28A and Lin28B interact with Dis3l2 exonuclease in the cytoplasm and that silencing of Dis3l2 upregulates uridylated pre-let-7 in both Lin28A-expressing and Lin28B-expressing cancer cell lines. Our findings collectively indicated that cytoplasmic uridylation pathway actively participates in blockade of let-7 biogenesis

© 2015 The Authors. Cancer Science published by Wiley Publishing Asia Pty Ltd on behalf of Japanese Cancer Association.

by Lin28B. In addition, although Lin28A is reported to act primarily in the cytoplasm, a recent report has shown that monomethylation of Lin28A by SET7/9 increases nuclear retention of Lin28A and induces blocking of pri-let-7 processing.[47] Thus, these studies suggest that Lin28A and Lin28B have considerably overlapping functions in the context of both uridylation-mediated cytoplasmic blockade and nuclear blockade of let-7 biogenesis.

Although localization of Lin28B is controversial,[20,21] a previous report suggests cell cycle-dependent dynamics of Lin28B, in which Lin28B accumulates in the nucleus in G2 and S phase.[8] In addition, Lin28A has also been reported to locate to stress granules upon cellular stress,[48] indicating dynamics of Lin28 localization. Interestingly, we found that amounts of let-7 may influence intracellular localization of Lin28B (Fig. 1f,g), suggesting that intracellular distribution of substrate RNA bound by Lin28 may alter the localization of Lin28A/B. Thus, various factors influence localization of Lin28 proteins, potentially explaining the controversy of Lin28B localization. Together with cytoplasmic localization of TUT4 and Dis3l2,[13,18,31,32] our findings support that cytoplasmic Lin28B blocks let-7 biogenesis in cooperation with uridylation pathway, including TUT4 and Di3l2.

We also found that MCPIP1 ribonuclease, involved in degradation of pre-miRNAs, is a secondary ribonuclase for degradation of uridylated pre-let-7 (Fig. 3). It has been shown that Lin28 promotes generation of uridylated pre-let-7 with heterogeneous length of uridine (U)-tail in cells expressing Lin28A or Lin28B.[6] Because Dis3l2 preferentially degrades long U-tails longer than 10 nucleotides,[17] a portion of uridylated pre-let-7 with short U-tails shorter than 10 nucleotides may not be efficient substrates for Dis3l2. Thus, it may be postulated that MCPIP1 degrades uridylated pre-let-7 with short U-tails and compensates for Dis3l2 activity in the uridylation pathway. In addition, considering that both Lin28B and MCPIP1 can be induced by inflammatory signals along with activation of NF-κB pathway,[37,39] coordinated regulation of MCPIP1 and Lin28B may reinforce the uridylation pathway to effectively block the biogenesis of let-7.

Furthermore, our analyses highlighted that Lin28B-positive cancers are associated with high expression of TUT4 and Dis3l2, supporting the positive contribution of uridylation pathway to Lin28B function. Because depletion of TUT4 has been shown to inhibit the growth of Lin28A-positive cancers,[20] our findings may expand the therapeutic potential of TUT4 inhibition to Lin28B-positive TUT4-high tumors. In addition, the present study suggests that Lin28A and Lin28B function as oncogenes in distinct cellular contexts affected by various factors, including cell types and Myc activation (Fig. 4d,e). Further analysis would provide insight into the pathological roles of Lin28A and Lin28B and their significance as potential biomarkers and therapeutic targets.

Acknowledgments

This work was supported by KAKENHI (Grants-in-Aid for Young Scientists (A) (No. 24689018, H.I.S.) and for Scientific Research on Innovative Areas "RNA regulation" (No. 23112702, H.I.S.)) from the Japan Society for the Promotion of Science and the Ministry of Education, Culture, Sports, Science, and Technology of Japan, and the Cell Science Research Foundation (H.I.S.). H.I.S. is a fellow of JSPS Postdoctoral Fellowship for Research Abroad. We thank M. Saitoh for supplying T47D cells. The results shown here are in part based upon data generated by the TCGA Research Network: http://cancergenome.nih.gov/. Information about TCGA and the investigators and institutions who constitute the TCGA research network can be found at http://cancergenome.nih.gov/.

Disclosure Statement

The authors have no conflict of interest to declare.

References

1 Suzuki HI, Miyazono K. Emerging complexity of microRNA generation cascades. *J Biochem* 2011; **149**: 15–25.
2 Suzuki HI, Miyazono K. Dynamics of microRNA biogenesis: crosstalk between p53 network and microRNA processing pathway. *J Mol Med (Berl)* 2010; **88**: 1085–94.
3 Newman MA, Thomson JM, Hammond SM. Lin-28 interaction with the Let-7 precursor loop mediates regulated microRNA processing. *RNA* 2008; **14**: 1539–49.
4 Viswanathan SR, Daley GQ, Gregory RI. Selective blockade of microRNA processing by Lin28. *Science* 2008; **320**: 97–100.
5 Rybak A, Fuchs H, Smirnova L *et al.* A feedback loop comprising lin-28 and let-7 controls pre-let-7 maturation during neural stem-cell commitment. *Nat Cell Biol* 2008; **10**: 987–93.
6 Heo I, Joo C, Cho J, Ha M, Han J, Kim VN. Lin28 mediates the terminal uridylation of let-7 precursor MicroRNA. *Mol Cell* 2008; **32**: 276–84.
7 Ouchi Y, Yamamoto J, Iwamoto T. The heterochronic genes lin-28a and lin-28b play an essential and evolutionarily conserved role in early zebrafish development. *PLoS One* 2014; **9**: e88086.
8 Guo Y, Chen Y, Ito H *et al.* Identification and characterization of lin-28 homolog B (LIN28B) in human hepatocellular carcinoma. *Gene* 2006; **384**: 51–61.
9 Yu J, Vodyanik MA, Smuga-Otto K *et al.* Induced pluripotent stem cell lines derived from human somatic cells. *Science* 2007; **318**: 1917–20.
10 Ma X, Li C, Sun L *et al.* Lin28/let-7 axis regulates aerobic glycolysis and cancer progression via PDK1. *Nat Commun* 2014; **5**: 5212.
11 Liu Y, Li H, Feng J *et al.* Lin28 induces epithelial-to-mesenchymal transition and stemness via downregulation of let-7a in breast cancer cells. *PLoS One* 2013; **8**: e83083.
12 Yang X, Lin X, Zhong X *et al.* Double-negative feedback loop between reprogramming factor LIN28 and microRNA let-7 regulates aldehyde dehydrogenase 1-positive cancer stem cells. *Cancer Res* 2010; **70**: 9463–72.
13 Heo I, Joo C, Kim Y *et al.* TUT4 in concert with Lin28 suppresses microRNA biogenesis through pre-microRNA uridylation. *Cell* 2009; **138**: 696–708.
14 Lehrbach NJ, Armisen J, Lightfoot HL *et al.* LIN-28 and the poly(U) polymerase PUP-2 regulate let-7 microRNA processing in *Caenorhabditis elegans*. *Nat Struct Mol Biol* 2009; **16**: 1016–20.
15 Hagan JP, Piskounova E, Gregory RI. Lin28 recruits the TUTase Zcchc11 to inhibit let-7 maturation in mouse embryonic stem cells. *Nat Struct Mol Biol* 2009; **16**: 1021–5.
16 Thornton JE, Chang HM, Piskounova E, Gregory RI. Lin28-mediated control of let-7 microRNA expression by alternative TUTases Zcchc11 (TUT4) and Zcchc6 (TUT7). *RNA* 2012; **18**: 1875–85.
17 Chang HM, Triboulet R, Thornton JE, Gregory RI. A role for the Perlman syndrome exonuclease Dis3l2 in the Lin28-let-7 pathway. *Nature* 2013; **497**: 244–8.
18 Ustianenko D, Hrossova D, Potesil D *et al.* Mammalian DIS3L2 exoribonuclease targets the uridylated precursors of let-7 miRNAs. *RNA* 2013; **19**: 1632–8.
19 Van Wynsberghe PM, Kai ZS, Massirer KB, Burton VH, Yeo GW, Pasquinelli AE. LIN-28 co-transcriptionally binds primary let-7 to regulate miRNA maturation in *Caenorhabditis elegans*. *Nat Struct Mol Biol* 2011; **18**: 302–8.
20 Piskounova E, Polytarchou C, Thornton JE *et al.* Lin28A and Lin28B inhibit let-7 microRNA biogenesis by distinct mechanisms. *Cell* 2011; **147**: 1066–79.
21 Hafner M, Max KE, Bandaru P *et al.* Identification of mRNAs bound and regulated by human LIN28 proteins and molecular requirements for RNA recognition. *RNA* 2013; **19**: 613–26.
22 Suzuki HI, Arase M, Matsuyama H *et al.* MCPIP1 ribonuclease antagonizes dicer and terminates microRNA biogenesis through precursor microRNA degradation. *Mol Cell* 2011; **44**: 424–36.

© 2015 The Authors. Cancer Science published by Wiley Publishing Asia Pty Ltd on behalf of Japanese Cancer Association.

23 Suzuki HI, Yamagata K, Sugimoto K, Iwamoto T, Kato S, Miyazono K. Modulation of microRNA processing by p53. *Nature* 2009; **460**: 529–33.
24 Matsuyama H, Suzuki HI, Nishimori H *et al.* miR-135b mediates NPM-ALK-driven oncogenicity and renders IL-17-producing immunophenotype to anaplastic large cell lymphoma. *Blood* 2011; **118**: 6881–92.
25 Suzuki HI, Matsuyama H, Noguchi M *et al.* Computational dissection of distinct microRNA activity signatures associated with peripheral T cell lymphoma subtypes. *Leukemia* 2013; **27**: 2107–11.
26 Barretina J, Caponigro G, Stransky N *et al.* The Cancer Cell Line Encyclopedia enables predictive modelling of anticancer drug sensitivity. *Nature* 2012; **483**: 603–7.
27 Subramanian A, Tamayo P, Mootha VK *et al.* Gene set enrichment analysis: a knowledge-based approach for interpreting genome-wide expression profiles. *Proc Natl Acad Sci U S A* 2005; **102**: 15545–50.
28 Gurtan AM, Ravi A, Rahl PB *et al.* Let-7 represses Nr6a1 and a mid-gestation developmental program in adult fibroblasts. *Genes Dev* 2013; **27**: 941–54.
29 Moss EG, Lee RC, Ambros V. The cold shock domain protein LIN-28 controls developmental timing in *C. elegans* and is regulated by the lin-4 RNA. *Cell* 1997; **88**: 637–46.
30 Yang DH, Moss EG. Temporally regulated expression of Lin-28 in diverse tissues of the developing mouse. *Gene Expr Patterns* 2003; **3**: 719–26.
31 Astuti D, Morris MR, Cooper WN *et al.* Germline mutations in DIS3L2 cause the Perlman syndrome of overgrowth and Wilms tumor susceptibility. *Nat Genet* 2012; **44**: 277–84.
32 Malecki M, Viegas SC, Carneiro T *et al.* The exoribonuclease Dis3L2 defines a novel eukaryotic RNA degradation pathway. *EMBO J* 2013; **32**: 1842–54.
33 Viswanathan SR, Powers JT, Einhorn W *et al.* Lin28 promotes transformation and is associated with advanced human malignancies. *Nat Genet* 2009; **41**: 843–8.
34 West JA, Viswanathan SR, Yabuuchi A *et al.* A role for Lin28 in primordial germ-cell development and germ-cell malignancy. *Nature* 2009; **460**: 909–13.
35 King CE, Cuatrecasas M, Castells A, Sepulveda AR, Lee JS, Rustgi AK. LIN28B promotes colon cancer progression and metastasis. *Cancer Res* 2011; **71**: 4260–8.
36 Suzuki HI, Miyazono K. Control of microRNA maturation by p53 tumor suppressor and MCPIP1 ribonuclease. *Enzymes* 2012; **32**: 163–83.
37 Iliopoulos D, Hirsch HA, Struhl K. An epigenetic switch involving NF-kappaB, Lin28, Let-7 MicroRNA, and IL6 links inflammation to cell transformation. *Cell* 2009; **139**: 693–706.
38 Matsushita K, Takeuchi O, Standley DM *et al.* Zc3h12a is an RNase essential for controlling immune responses by regulating mRNA decay. *Nature* 2009; **458**: 1185–90.
39 Jura J, Skalniak L, Koj A. Monocyte chemotactic protein-1-induced protein-1 (MCPIP1) is a novel multifunctional modulator of inflammatory reactions. *Biochim Biophys Acta* 2012; **1823**: 1905–13.
40 Thornton JE, Gregory RI. How does Lin28 let-7 control development and disease? *Trends Cell Biol* 2012; **22**: 474–82.
41 Urbach A, Yermalovich A, Zhang J *et al.* Lin28 sustains early renal progenitors and induces Wilms tumor. *Genes Dev* 2014; **28**: 971–82.
42 Molenaar JJ, Domingo-Fernandez R, Ebus ME *et al.* LIN28B induces neuroblastoma and enhances MYCN levels via let-7 suppression. *Nat Genet* 2012; **44**: 1199–206.
43 Diskin SJ, Capasso M, Schnepp RW *et al.* Common variation at 6q16 within HACE1 and LIN28B influences susceptibility to neuroblastoma. *Nat Genet* 2012; **44**: 1126–30.
44 Charafe-Jauffret E, Ginestier C, Monville F *et al.* Gene expression profiling of breast cell lines identifies potential new basal markers. *Oncogene* 2006; **25**: 2273–84.
45 Pujana MA, Han JD, Starita LM *et al.* Network modeling links breast cancer susceptibility and centrosome dysfunction. *Nat Genet* 2007; **39**: 1338–49.
46 Chang TC, Zeitels LR, Hwang HW *et al.* Lin-28B transactivation is necessary for Myc-mediated let-7 repression and proliferation. *Proc Natl Acad Sci U S A* 2009; **106**: 3384–9.
47 Kim SK, Lee H, Han K *et al.* SET7/9 methylation of the pluripotency factor LIN28A is a nucleolar localization mechanism that blocks let-7 biogenesis in human ESCs. *Cell Stem Cell* 2014; **15**: 735–49.
48 Balzer E, Moss EG. Localization of the developmental timing regulator Lin28 to mRNP complexes, P-bodies and stress granules. *RNA Biol* 2007; **4**: 16–25.

Supporting Information

Additional supporting information may be found in the online version of this article:

Fig. S1. Inhibition of let-7 function and biogenesis by MCPIP1 in HEK293T cells. (a) Effect of MCPIP1 on let-7g activity in HEK293T cells. Let-7g sensor and pri-let-7g were coexpressed with/without MCPIP1 (wild type [WT], D141N and C306R) in HEK293T cells, and subjected to luciferase reporter assay. (b) Suppression of let-7 biogensis by MCPIP1. HEK293T cells were cotransfected with MCPIP1 expression vector and pri-let-7g expression vector, and applied to qRT-PCR analysis. Error bars represent SD. $*P < 0.05$

Fig. S2. An association between Lin28 and uridylation pathway in Cancer Cell Line Encyclopedia (CCLE) database. (a,b) Upregulation of let-7 potential target genes and high confidence target genes in Lin28A-positive (a) and Lin28B-positive (b) cell lines in CCLE, analyzed by using gene set enrichment analysis (GSEA). (c) Upregulation of let-7 potential target genes in TUT4-high Lin28B-positive cell lines in CCLE, compared to TUT4-low Lin28B-positive cell line, analyzed by GSEA.

Fig. S3. Effects of Lin28B on let-7 family members in TCGA hepatocellular carcinoma database. (top) Comparison of sequences of precursors of let-7 family miRNAs. (bottom) Violin plots of Z-scores for expression levels for independent let-7 family miRNAs in TCGA hepatocellular carcinoma database. Boxes represent the median and IQR. Error bars represent 1.5× IQR.

Table S1. Primers used in this study.

Table S2. Lead edge genes in high confidence let-7 target gene set, which are overexpressed in Lin28B + TUT4 high cancer cell lines.

Table S3. Gene set enrichment analysis (GSEA) results in Cancer Cell Line Encyclopedia (CCLE) dataset (C2CGP gene sets).

Table S4. Gene set enrichment analysis (GSEA) results in Cancer Cell Line Encyclopedia (CCLE) dataset (Hallmark gene sets).

© 2015 The Authors. Cancer Science published by Wiley Publishing Asia Pty Ltd on behalf of Japanese Cancer Association.